



Published in final edited form as:

*Mucosal Immunol.* 2014 November ; 7(6): 1366–1374. doi:10.1038/mi.2014.24.

## Secretion of IL-16 through TNFR1 and calpain-caspase signaling contributes to MRSA pneumonia

Danielle Ahn<sup>1</sup>, Dane Parker<sup>1</sup>, Paul J. Planet<sup>1</sup>, Pamela A. Nieto<sup>3,4</sup>, Susan M. Bueno<sup>3,4</sup>, and Alice Prince<sup>1,2,\*</sup>

<sup>1</sup>Departments of Pediatrics, Columbia University College of Physicians and Surgeons, New York, New York, USA

<sup>2</sup>Department of Pharmacology, Columbia University College of Physicians and Surgeon, New York, New York, USA

<sup>3</sup>Millennium Institute on Immunology and Immunotherapy, Santiago, Chile

<sup>4</sup>Departamento de Genética Molecular y Microbiología, Facultad de Ciencias Biológicas, Pontificia Universidad Católica de Chile, Santiago, Chile

### Abstract

*Staphylococcus aureus* is a major cause of severe pneumonia. Multiple mechanisms of proinflammatory signaling are activated to recruit immune cells into the airway in response to *S. aureus*. We found that IL-16, a T cell cytokine that binds CD4, is potently activated by *S. aureus*, specifically by protein A (SpA), and to a much greater extent than by Gram negative pathogens or LPS. IL-16 production involved multiple signals including ligation of TNFR family members or EGFR, both receptors for SpA and generation of Ca<sup>2+</sup> fluxes to activate calpains and caspase-3. Although human airway epithelial cells, vascular endothelial cells, THP-1 and Jurkat T cells released IL-16 in response to *S. aureus* in vitro, in a murine model of pneumonia, CD4<sup>+</sup> cells were the major source of IL-16 suggesting the involvement of an autocrine signaling pathway. The production of IL-16 contributed to lung damage as neutralization of IL-16 enhanced *S. aureus* clearance and resulted in diminished lung pathology in *S. aureus* pneumonia. Our results suggest that the ability of *S. aureus* to activate TNFR1 and Ca<sup>2+</sup>/calpain signaling contribute to T cell activation and excessive inflammation in the setting of acute pneumonia.

### INTRODUCTION

*Staphylococcus aureus*, particularly the epidemic USA300 methicillin-resistant *S. aureus* (MRSA), is a major cause of pneumonia<sup>1</sup>. Common in health care associated settings, MRSA is a frequent cause of ventilator-associated pneumonia<sup>2</sup> and superinfection complicating influenza<sup>3</sup>. Even though there are antimicrobials with good activity against

Users may view, print, copy, and download text and data-mine the content in such documents, for the purposes of academic research, subject always to the full Conditions of use:[http://www.nature.com/authors/editorial\\_policies/license.html#terms](http://www.nature.com/authors/editorial_policies/license.html#terms)

\* corresponding author BB 416 650 W. 168<sup>th</sup> St New York, NY 10032 212 305-4193 asp7@columbia.edu.

#### DISCLOSURES

The authors declare no conflict of interest.

MRSA, there remains significant morbidity and mortality associated with this pathogen<sup>1,4</sup>. A substantial literature suggests that specific staphylococcal virulence factors are directly responsible for lung injury such as  $\alpha$ -hemolysin (hla)<sup>5</sup> and Panton-Valentine leukocidin (PVL)<sup>6</sup>. However, much of the pathology associated with MRSA pneumonia can be attributed to the intensity of the host inflammatory response. *S. aureus* activates multiple redundant proinflammatory signaling cascades and murine models of *S. aureus* pneumonia lacking specific components of the innate immune signaling pathway such as type 1 interferon receptor<sup>7</sup>, inflammasome protein NLRP3<sup>8</sup> and TNF receptor 1 (TNFR1)<sup>9</sup> have improved bacterial clearance. *S. aureus* infection is accompanied by a significant TNF response and the abundant *S. aureus* surface component protein A (SpA), directly activates TNFR1 signaling<sup>10</sup>.

The recruitment of neutrophils and macrophages in response to chemokine and cytokine expression in the lung is a critical component of innate immune signaling in response to *S. aureus*<sup>11,12</sup>. The contribution of T cells in the setting of acute staphylococcal infection is less well characterized, but is likely to be important<sup>13</sup> as seen in *Rag2*<sup>-/-</sup> mice, which exhibited resistance to *S. aureus* infection in a sepsis model<sup>14</sup>. Not only are T cells essential to coordinate an adaptive immune response, they can be directly activated by *S. aureus* superantigens and are a major source of proinflammatory cytokines<sup>15</sup>, such as TNF. Activated T cells contribute to pulmonary pathology in the setting of acute lung injury. CXCR3 is preferentially expressed in T<sub>H</sub>1 cells<sup>16</sup>, and is increased in both infectious and noninfectious models of acute lung injury<sup>11,12</sup>.

Overexpression of the T cell chemokine CXCL10, a CXCR3 ligand, induced airway inflammation<sup>16</sup> and infected CXCL10 KO mice had decreased lung pathology<sup>11</sup>. In acute bacterial infection, multiple T cell chemokines and cytokines are produced such as IL-12<sup>17</sup> and IL-16<sup>18</sup>, which serve to recruit T cells and stimulate the expression of surface receptors that mediate their proliferation and cytokine production.

IL-16 is a multifunctional cytokine with a single PDZ domain initially characterized as a product of human peripheral blood mononuclear cells and described as a lymphocyte chemoattractant<sup>19</sup> (previously named lymphocyte chemoattractant factor). Transcribed as pro-IL-16, its production is regulated both at the level of transcription and caspase-3 dependent processing in various cell types<sup>18</sup>. IL-16 induces chemotaxis of CD4<sup>+</sup> cells such as lymphocytes, eosinophils and dendritic cells by ligating CD4 directly at a site distinct from other ligands<sup>18,19</sup>. Among its multiple functions, IL-16 is a T cell chemoattractant involved in T<sub>H</sub>1 inflammatory responses and the regulation of both T cell growth and responsiveness to regulatory cytokines<sup>20</sup>. Chemotaxis of T cells induced by the supernatant of TNF-stimulated epithelial cells is inhibited by anti-IL-16 antibody<sup>21</sup>, indicating a close association between IL-16 and TNF signaling. The processing of pro-IL-16 to its active form is mediated by caspase-3<sup>22</sup> via caspase-8. These caspases are activated following ligation of TNFR1<sup>23</sup>, the target of SpA<sup>10</sup>. In inflammatory conditions characterized by excessive TNF signaling, such as inflammatory bowel disease, IL-16 contributes significantly to pathology<sup>24</sup>, thus we postulate that in the setting of robust TNF signaling, as occurs during *S. aureus* pneumonia, IL-16 similarly contributes to pathology.

In the experiments detailed herein, we describe the participation of IL-16 in *S. aureus* pneumonia and suggest that the unique ability of this organism to directly activate TNFR1, as well as the Ca<sup>2+</sup>/calpain/caspase cascade, results in release of this T cell cytokine.

## RESULTS

### *S. aureus* induces IL-16 in the murine lung

Significantly higher levels of IL-16 were recovered from the bronchoalveolar lavage fluid (BALF) of WT mice infected with 10<sup>7</sup> cfu methicillin resistant *S. aureus* USA300 (MRSA) strain (p=0.0001 compared to PBS) or *S. aureus* 502A, a representative methicillin sensitive strain. Lower levels were retrieved from mice infected with 10<sup>7</sup> cfu of Gram negative organisms such as *Klebsiella pneumoniae* ST 258 and *Pseudomonas aeruginosa* PAK (p<0.05 compared to MRSA) (**Figure 1a**). To determine if human cells similarly had differential IL-16 responses to *S. aureus* versus Gram negative stimuli the human monocytic cells, THP-1s were stimulated with the same pathogens. IL-16 from THP-1s was 18-fold higher than the media control after incubation with MRSA (p=0.0001) and 20-fold after infection with *S. aureus* 502A. Less IL-16 was measured in response to infection with Kp or PAK (p<0.05 compared to MRSA) (**Figure 1b**).

### IL-16 secretion is SpA dependent in specific cell types

The major *S. aureus* surface component SpA activates TNFR1 signaling<sup>10</sup>, a receptor expected to activate IL-16 processing. The ability of the WT MRSA, a *spa* null mutant, and purified SpA to stimulate IL-16 in several cell types was compared (**Figure 2**). Induction of IL-16 by the *spa* null mutant was significantly decreased as compared to MRSA in human bronchial epithelial cells (16HBEs) (p=0.028) (**Figure 2a**), human umbilical vein endothelial cells (HUVECs) (p=0.002) (**Figure 2b**) and T cells (Jurkats) (p=0.06) (**Figure 2c**); WT MRSA and the *spa* null mutant stimulated similar amounts of IL-16 in monocytes (THP-1s) (**Figure 2d**). SpA alone induced IL-16 release from 16HBEs, HUVECs, Jurkats and THP-1s (all p<0.05 as compared to media alone). Of note, LPS and TNF failed to stimulate IL-16 secretion in any of the cell types tested, with the exception of TNF stimulated Jurkats (p<0.05 as compared to media).

### TNFR1 participates in IL-16 secretion

TNFR1 ligation activates caspase-3 signaling<sup>23</sup>, important in the processing of pro-IL-16 to its active form<sup>22</sup> and is stimulated by the IgG binding domain of SpA<sup>10</sup>. To establish the importance of TNFR1 mediated signaling in the induction of IL-16 production, we compared generation of IL-16 in WT and *Tnfr1*<sup>-/-</sup> mice (**Figure 3**). There was significantly less IL-16 in the BALF of infected *Tnfr1*<sup>-/-</sup> mice compared to WT controls (p<0.05) (**Figure 3a**). Protein content in the BALF was slightly lower in the KO mice (**Figure 3b**) with similar levels of KC (**Figure 3c**). Histopathology of *Tnfr1*<sup>-/-</sup> lungs infected with MRSA suggested less destruction of the normal architecture than WT mouse lung (**Figure 3d**), consistent with previous reports<sup>10</sup>. Numbers of bacteria recovered in BALF were similar (**Figure 3e**) and recruited innate immune cells into BALF and lung were not significantly different in the WT and *Tnfr1*<sup>-/-</sup> mice (**Figure 3f-h**). Participation of TNFR1

in IL-16 processing is evident, but incomplete attenuation of IL-16 production in *Tnfr1*<sup>-/-</sup> mice suggests that other pathways are involved.

### Multiple receptors participate in MRSA induced IL-16 secretion

The direct association of SpA and IL-16 shown in stromal and T-cells, indicates that additional SpA receptors may be involved in the generation of IL-16. Accordingly, we tested the participation of EGF receptor (EGFR), a receptor for the IgG binding domain of SpA and directly activated in *S. aureus* infection<sup>25</sup>. In the presence of blocking antibody to EGFR, MRSA induction of IL-16 secretion in THP-1s was significantly diminished ( $p=0.023$ ) as compared to an relevant IgG control (**Figure 4a**). Activation of FasL (CD95), another member of the TNFR superfamily<sup>23</sup>, also leads to pro-caspase-8 cleavage<sup>26</sup>, which in turn activates caspase-3 from its proform, by  $Ca^{2+}$  influx and calpain activation<sup>27</sup>. Pre-treatment of THP-1s with anti-FasL antibody prior to infection with MRSA also diminished the release of IL-16 ( $p=0.0007$ ) (**Figure 4b**). As  $Ca^{2+}$  fluxes are generated by TLR2 signaling<sup>28</sup>, induced by *S. aureus*<sup>29</sup>, we monitored IL-16 production by THP-1s pre-treated with anti-TLR2 and found no diminution of IL-16 levels (**Figure 4c**). In addition, incubation of THP-1s with the TLR2 agonist Pam<sub>3</sub>Cys-Ser-Lys<sub>4</sub> did not induce IL-16 production, indicating that TLR2 by itself is not responsible for IL-16 production. Thus, multiple TNFR effectors, as well as EGFR, participate in IL-16 secretion.

### Calcium, calpains and caspases are involved in IL-16 processing

Our results suggest that multiple ligands that activate caspase-8 and caspase-3 could participate in the induction of pro-IL-16 processing<sup>22</sup>. Given the participation of the  $Ca^{2+}$ -dependent calpains in caspase activation, we examined the requirement of  $Ca^{2+}$  fluxes in the induction of IL-16. MRSA induced  $Ca^{2+}$  fluxes in Flo-4/AM loaded THP-1s within 10 min of exposure to MRSA with attenuation by pretreatment with BAPTA (**Figure 5a** and **Supplementary Figure S1a-b**). THP-1s in media alone showed no baseline  $Ca^{2+}$  fluxes and gave significant fluorescence when treated with thapsigargin (**Figure 5b** and **Supplementary Figure S1c**). IL-16 secretion was stimulated by ionomycin alone and significantly decreased in the presence of EDTA ( $p<0.05$  compared to media) (**Figure 5c**). Pretreatment of THP-1s with calpeptin, a calpain inhibitor, resulted in diminished secretion of IL-16 ( $p<0.05$  compared to DMSO) (**Figure 5d**), indicating that IL-16 processing in THP-1s is calpain, as well as calcium dependent. Similar differences in Jurkats with calcium and calpain inhibitors were not seen (data not shown). Caspase-3 involvement was demonstrated when THP-1s preloaded with Caspase-3/7 Green Detection Reagent were infected with MRSA, showing an increase in fluorescence over baseline (**Figure 5e**). We then observed decreased secretion of IL-16 when THP-1s were pretreated with pancaspase inhibitor Z-VAD-FMK ( $p<0.05$  compared to DMSO with MRSA) or a caspase-3 inhibitor ( $p<0.05$  compared to DMSO with MRSA) but not a caspase-1 inhibitor (**Figure 5f**). Similarly, IL-16 release was reduced in Jurkats pretreated with caspase-3 inhibitor ( $p<0.05$  compared to DMSO with MRSA) (**Figure 5g**). Staurosporine control, an *in vitro* inducer of caspase activity<sup>30</sup>, showed induction of IL-16 secretion in both THP-1s and Jurkats.

## T cells are a major source of IL-16

Our *in vitro* data suggest that multiple cells types can produce IL-16. To determine the major source of IL-16 in the setting of *S. aureus* pneumonia, immunohistochemistry was performed on lung sections of WT mice infected with MRSA. IL-16 staining was observed in discrete cells (black arrows), and not a generalized response of the respiratory epithelium in MRSA infection (**Figure 6a**). Since CD4 itself is a receptor for IL-16, we predicted that CD4<sup>+</sup> cells would participate in an autocrine loop and were a likely source of the cytokine in the lung. *Cd4*<sup>-/-</sup> and WT mice were infected with MRSA, and at 24 hours post inoculation, IL-16 in the BALF was nearly half in the airway of the *Cd4*<sup>-/-</sup> mouse compared to WT counterparts (p=0.0043) (**Figure 6b**). The apparent correlation between the abundance of CD4<sup>+</sup> cells and IL-16 production was further confirmed in MRSA infected mice with increased numbers of CD4<sup>+</sup> cells. We noted that mice treated with clodronate, depleted of alveolar macrophages had a significant increase in the numbers of pulmonary CD4<sup>+</sup> cells (**Figure 6c**), but not other T-cell populations<sup>12</sup>. These mice had a corresponding increase in IL-16 in the setting of MRSA pneumonia (**Figure 6d**), suggesting CD4<sup>+</sup> cells are stimulated by, as well as generate IL-16 in an autocrine manner.

## Neutralization of IL-16 improves clearance of MRSA and pathology

The exuberant host response to infection is a hallmark of *S. aureus* pneumonia and we postulated that neutralization of IL-16 would dampen its harmful consequences. By directly affecting CD4<sup>+</sup> cells, we hypothesized that we might limit the excessive proinflammatory response, without compromising the recruitment of phagocytes essential to clear infection. As mice lacking IL-16 production are not available, we pretreated mice with anti-IL-16 before giving our standard intranasal inoculum of MRSA, documenting the expected reduction in the amount of IL-16 in the airway as compared to IgG control (p=0.04) (**Figure 7a**). A major effect on MRSA clearance was observed with a 6-fold reduction in cfus recovered from the airways (p=0.0042) (**Figure 7b**) and better preservation of the normal lung architecture, than in the IgG-treated control (**Figure 7c**). Decreased amounts of KC (p=0.016) were seen in the neutralization group (**Figure 7d**), but the cellular populations recruited to the BALF and lung were unaffected (**Supplemental Figure S2a-h**). TNF, IL 6 and protein levels were similar (**Figure 7e-g**). Thus, IL-16 contributes to lung pathology in MRSA pneumonia.

## DISCUSSION

IL-16 has been described in a number of inflammatory and oncologic conditions since its description by Cruikshank in 1982<sup>31</sup>. However, despite its importance in the development of T<sub>H</sub>1-mediated inflammation<sup>32</sup>, relatively little is known about its role in the pathogenesis of bacterial infection, including *S. aureus* pneumonia<sup>33</sup>. The biology of murine and human IL-16 is highly conserved<sup>34</sup>, thus the analysis of IL-16 in murine models of infection is likely applicable in human tissues as well. IL-16, as a ligand for CD4<sup>+</sup> cells, functions in T cell activation as well as proliferation<sup>35</sup> and has biologic activity in both its pro-form and mature processed form<sup>36</sup>. We demonstrate that MRSA induces IL-16 acutely in the lung, where it participates in the exuberant and potentially damaging inflammatory response to infection.

Multiple cell types contribute to the proinflammatory signaling produced in response to *S. aureus* with the production of NF- $\kappa$ B dependent cytokines and chemokines<sup>37</sup>. Epithelial, endothelial and immune cells can all produce IL-16 as part of the immediate response to MRSA. However, in contrast to the NF- $\kappa$ B dependent cytokines, IL-16 production appears to be specifically linked to the TNF cascade and dependent upon both TNF and specific bacterial ligands. LPS and TNF alone failed to stimulate IL-16 production, whereas MRSA and SpA alone were potent stimuli in most of the cell types examined. The central role of the TNF cascade in the induction of IL-16 processing, as demonstrated by diminished IL-16 production in infected mice lacking TNFR1, suggests an explanation for the enhanced ability of MRSA to activate this cytokine. In addition to stimulating TNF indirectly through production of PAMPs and pattern recognition receptors on immune cells, SpA directly ligates both TNFR1 and EGFR on multiple cell types to initiate signaling<sup>10,25</sup> through redundant signaling pathways. IL-16 secretion into the airway of infected mice lacking TNFR1 was not fully attenuated and signaling by multiple receptors, including EGFR and FasL, were found to initiate the processing of IL-16 to its active form.

A second stimulus, the generation of a Ca<sup>2+</sup> flux sufficient to activate calpain activity was also required for IL-16 production. We demonstrated this response in THP-1s, representative of alveolar macrophages, the predominant immune cell to initially encounter respiratory pathogens. We were unable to show this calcium dependence in Jurkats, as Ca<sup>2+</sup> fluxes are readily activated in T cells<sup>38</sup>, which also possess the CD4 receptor for IL-16. *In vivo*, these CD4<sup>+</sup> cells appear to be the most responsive to the multiple stimuli apparently required to initiate IL-16 processing. *In vitro*, we and others<sup>18</sup> have demonstrated that multiple cell types can produce IL-16. However, the requirement for TNF signaling or ligation of a TNFR family receptor plus the need for calpain activity likely limits the *in vivo* production of the cytokine to specific cell types. This requirement for multiple stimuli may also help to explain why LPS alone, or the Gram negative airway pathogens tested were much less capable in stimulating IL-16 production.

Once T cells are recruited, IL-16 CD4 interactions initiate an autocrine loop to further induce T cell production of more IL-16. The ability of *S. aureus* to directly initiate a T cell cytokine response may contribute to virulence. The improved MRSA clearance in mice with decreased IL-16 suggests that T cell recruitment and activation may contribute to lung damage in this setting. In our murine model system, we were unable to detect differences in numbers of the major immune cells recruited in mice treated with anti-IL-16 or the isotype control. Thus, the effects of the anti-IL-16 may be in blocking further T-cell activity and their contribution to cytokine production.

In several other murine models of bacterial pneumonia, the ability to clear infection and preserve lung architecture correlated with decreased cytokine expression and not with the absolute numbers of inflammatory cells recruited into the lung<sup>39,40</sup>. There are multiple potential sources of neutrophil and macrophage chemokines<sup>37,41</sup>. Limiting the participation of IL-16 and its T cell targets did not limit phagocytic influx, but resulted in decreased production of KC. Of note, KC is a major neutrophil chemokine that has been linked to lung injury in other models of sepsis<sup>42,43</sup> consistent with the hypothesis that cytokines themselves, may be directly associated with lung damage.

In the absence of an *Il16*<sup>-/-</sup> mouse it is difficult to fully evaluate the role of this cytokine in the acute response to MRSA pneumonia. Our data indicate that the capability of MRSA, as opposed to commensal or opportunistic Gram negative airway pathogens, to activate IL-16 and initiate this amplification of CD4<sup>+</sup> T cell participation further contributes to its virulence in the setting of pneumonia.

## METHODS

### Cell culture, bacterial strains, and purified proteins

Human airway epithelial cells (16HBEs, D. Gruenert, California Pacific Medical Center Research Institute, San Francisco, CA), human umbilical vein endothelial cells in primary culture (HUVECs, B. Hopkins, Columbia College of Physicians and Surgeons, New York, NY), THP-1 human monocytic cells (THP-1s, ATCC, Manassas, VA), and Jurkat human T-cells (Jurkats, E6-1, ATCC, Manassas, VA) were grown at 37°C with 5% CO<sub>2</sub>. THP-1s were activated with 1 μM phorbol 12-myristate 13-acetate (PMA) and Jurkats were activated with 0.1 μM PMA + 0.1 μM ionomycin, both for 24 hours prior to infection. Methicillin resistant *S. aureus* USA300 (MRSA)<sup>44</sup>, isogenic *spa* mutant<sup>7</sup>, *S. aureus* 502A, *K. pneumoniae* ST 258 and *P. aeruginosa* PAK were grown in LB and resuspended in antibiotic free media (16HBEs – Bronchiolife, Lifeline Technologies, HUVECs – Vasculife, Lifeline Technologies or THP-1s/Jurkats – RPMI, Corning, with 10% heat inactivated fetal bovine serum, Benchmark) for infections *in vitro*. Purified SpA (Calbiochem) and TNF (Peprotech) were added at differential concentrations based on the assay. Pam<sub>3</sub>Cys-Ser-Lys<sub>4</sub> (EMC Microcollections), thapsigargin (Invitrogen), ionomycin (Calbiochem) and staurosporine (Cell Signaling) were used as positive controls in respective assays.

### Antibodies and Inhibitors

Antibodies used *in vitro* were anti-EGFR (1005; Santa Cruz), anti-FasL (NOK1; BD Biosciences), anti-TLR2 (H 175; Santa Cruz), anti-TNFR1 (H-271; Santa Cruz) and anti-IL-16 (ab9563; Abcam). Respective IgG isotype controls were used for comparison; rabbit (2027; Santa Cruz) or mouse (2025; Santa Cruz). Inhibitors used were pancaspase inhibitor ZVAD-FMK (Santa Cruz), caspase-3 inhibitor (Calbiochem), caspase 1 inhibitor (Calbiochem), calpeptin (Calbiochem), BAPTA (Calbiochem) and EDTA (Sigma).

### Mouse studies

*In vivo* experiments were performed using age and sex-matched WT, *Tnfr1*<sup>-/-</sup>, and *Cd4*<sup>-/-</sup> C57BL/6J mice (Jackson Laboratories). Mice were anaesthetized with 100 mg/kg ketamine and 5 mg/kg xylazine, infected intranasally with MRSA, *S. aureus* 502A, *K. pneumoniae* ST 258 or *P. aeruginosa* PAK (10<sup>7</sup> cfu in 50 QL of PBS), and sacrificed 18-24 hours after infection. To deplete macrophages, 75 QL of clodronate liposomes or PBS liposome controls were inoculated intranasally 24 hours prior to infection with MRSA as previously described<sup>12</sup>. For the neutralization of IL-16, 100 μg of anti-IL-16 antibody (ab9563; Abcam) or IgG isotype (Jackson ImmunoResearch) was injected intraperitoneally 2 hours prior to infection as previously described<sup>45</sup>. Animal experiments were performed in accordance with the guidelines of the IACUC at Columbia University (protocol number AAAE5252 and AAAD0624).

### Bronchoalveolar Lavage Fluid (BALF) Assays

BALF was obtained by instilling 1 mL aliquots of sterile PBS with calcium and magnesium into a cannulated trachea three times. Serial dilutions for bacterial enumeration were performed on the BALF prior to centrifuging. IL-16 mouse ELISA (R&D Systems), TNF mouse ELISA (eBioscience), KC mouse ELISA (R&D systems), IL 6 mouse ELISA (Biolegend), and Bradford Assay (Thermo Scientific) for protein content were performed on the BALF supernatant.

### Analysis of immune cell populations

Analysis of cell populations in BALF or single cell suspension of lung homogenate was conducted as before<sup>46</sup>. Cells were labeled with a combination of phycoerythrin (PE)-labeled anti-NK 1.1 (PK136; eBioscience), fluorescein (FITC)-labeled anti-Ly6G (RB6-8C5; eBioscience), allophycocyanin (APC)-labeled anti-MHCII (M5/114.15.2; eBioscience), PerCP-Cy5.5-labelled anti-CD11c (N418; Biolegend), or phycoerythrin (PE)-labeled CD4 (RM4-5; Biolegend) alone. Neutrophils (PMNs) were defined as Ly6G<sup>+</sup>/MHCII<sup>-</sup>, Macrophages as CD11c<sup>+</sup>/MHCII<sup>low-mid</sup> and Dendritic cells (DCs) as CD11c<sup>+</sup>/MHCII<sup>high</sup>. Fc block (anti-mouse CD16/32) was also added to each sample (93; eBioscience). Uniform dyed microspheres (Bangs Laboratories, Inc) were added to calculate the concentration of cellular components. Samples were run on FACS Calibur and analyzed on FlowJo (ver 10.0.6).

### Histopathology and Immunohistochemistry

Whole mouse lung was fixed with 4% paraformaldehyde for 24 hours, 70% ethanol for 24 hours, and then prepared in paraffin blocks. H&E staining was performed on 5 mm sections for gross pathology. For immunohistochemistry (IHC), 5 mm sections on glass slides were rehydrated with xylene alternative (Safe Clear, Protocol) and ethanol. Antigens were presented using an acidic buffer (sodium citrate 10mM, 0.05% Tween 20, pH 6) at 60°C overnight. Sections were additionally permeabilized with Tween 20 0.5% for 10 minutes and quenched with 0.3% H<sub>2</sub>O<sub>2</sub> for 10 minutes. Detection of IL-16 by IHC with peroxidase staining was performed using the Immunocruz ABC Staining kit (Santa Cruz). Controls were performed with secondary antibody only.

### Calcium Imaging

THP-1s were loaded with AM/Flo-4 (Invitrogen) with PowerLoad concentrate (Invitrogen) prior to imaging and stimulation. Cells were imaged on an Olympus 1X81 inverted microscope with a GFP mercury laser. Images were analyzed and videos made using MetaMorph software (Ver.7.5.3.0, April, 2008).

### Caspase-3/7 Detection Assay

THP-1s were preloaded with CellEvent Caspase-3/7 Green Detection Reagent (Invitrogen) 30 minutes prior to infection. Cells were stimulated and then read at absorption/emission maxima of 502/530 nm every 10 minutes for 2 hours on a Tecan Infinite 200 (V2.11, April, 2008).

## Statistics

All statistical analysis was performed using GraphPad Prism Version 6.0c (March 21, 2013). Samples with normal distributions, were analyzed by Student's *t* test. Mouse samples were compared using the nonparametric Mann-Whitney test. For multiple comparisons, an ANOVA was then followed by a post hoc Dunnett's test to compare to the control group. Differences in groups were considered significant if  $p < 0.05$ .

## Supplementary Material

Refer to Web version on PubMed Central for supplementary material.

## ACKNOWLEDGEMENTS

This work was funded by R01HL079395 to AP. Fluorescence microscopy was performed in the laboratory of Jahar Bhattacharya with the gracious assistance of Kristen Westphalen at the Columbia University College of Physicians and Surgeons, New York, New York, USA.

## REFERENCES

1. Klevens RM, et al. Invasive Methicillin-Resistant *Staphylococcus aureus* Infections in the United States. *JAMA*. 2007; 298:1763–1771. [PubMed: 17940231]
2. Guidelines for the Management of Adults with Hospital-acquired, Ventilator-associated, and Healthcare associated Pneumonia. *Am. J. Respir. Crit. Care Med*. 2005; 171:388–416. [PubMed: 15699079]
3. Morens DM, Taubenberger JK, Fauci AS. Predominant Role of Bacterial Pneumonia as a Cause of Death in Pandemic Influenza: Implications for Pandemic Influenza Preparedness. *J. Infect. Dis*. 2008; 198:962–970. [PubMed: 18710327]
4. Kollef MH, et al. Epidemiology and Outcomes of Health-care–Associated Pneumonia Results From a Large US Database of Culture-Positive Pneumonia. *Chest*. 2005; 128:3854–3862. [PubMed: 16354854]
5. Inoshima I, et al. A *Staphylococcus aureus* pore-forming toxin subverts the activity of ADAM10 to cause lethal infection in mice. *Nat. Med*. 2011; 17:1310–1314. [PubMed: 21926978]
6. Diep BA, et al. Polymorphonuclear leukocytes mediate *Staphylococcus aureus* Panton-Valentine leukocidin-induced lung inflammation and injury. *Proc. Natl. Acad. Sci. U. S. A*. 2010; 107:5587–5592. [PubMed: 20231457]
7. Martin FJ, Gomez MI, Wetzel DM, Memmi G, O'Seaghda M, Soong G, Schindler C, Prince A. *Staphylococcus aureus* activates type I IFN signaling in mice and humans through the Xr repeated sequences of protein A. *J. Clin. Invest*. 2009; 119:1931–1939. [PubMed: 19603548]
8. Kebaier C, et al. *Staphylococcus aureus*  $\alpha$ -Hemolysin Mediates Virulence in a Murine Model of Severe Pneumonia Through Activation of the NLRP3 Inflammasome. *J. Infect. Dis*. 2012; 205:807–817. [PubMed: 22279123]
9. Gomez MI, et al. *Staphylococcus aureus* protein A induces airway epithelial inflammatory responses by activating TNFR1. *Nat. Med*. 2004; 10:842–848. [PubMed: 15247912]
10. Gomez MI. *Staphylococcus aureus* Protein A Activates TNFR1 Signaling through Conserved IgG Binding Domains. *J. Biol. Chem*. 2006; 281:20190–20196. [PubMed: 16709567]
11. Ichikawa A, et al. CXCL10-CXCR3 enhances the development of neutrophil mediated fulminant lung injury of viral and nonviral origin. *Am. J. Respir. Crit. Care Med*. 2013; 187:65–77. [PubMed: 23144331]
12. Martin FJ, Parker D, Harfenist BS, Soong G, Prince A. Participation of CD11c(+) leukocytes in methicillin resistant *Staphylococcus aureus* clearance from the lung. *Infect. Immun*. 2011; 79:1898–1904. [PubMed: 21402768]

13. McLoughlin RM, et al. CD4+ T cells and CXC chemokines modulate the pathogenesis of *Staphylococcus aureus* wound infections. Proc. Natl. Acad. Sci. U. S. A. 2006; 103:10408–10413. [PubMed: 16801559]
14. Köckritz-Blickwede, von, M., et al. Immunological Mechanisms Underlying the Genetic Predisposition to Severe *Staphylococcus aureus* Infection in the Mouse Model. Am. J. Pathol. 2008; 173:1657–1668. [PubMed: 18974303]
15. Wilson GJ, et al. A Novel Core Genome-Encoded Superantigen Contributes to Lethality of Community-Associated MRSA Necrotizing Pneumonia. PLoS Pathog. 2011; 7:e1002271. [PubMed: 22022262]
16. Jiang D, et al. Long-term exposure of chemokine CXCL10 causes bronchiolitis-like inflammation. Am. J. Respir. Cell Mol. Biol. 2012; 46:592–598. [PubMed: 22162905]
17. Hamza T, Barnett JB, Li B. Interleukin 12 a Key Immunoregulatory Cytokine in Infection Applications. Int. J. Mol. Sci. 2010; 11:789–806. [PubMed: 20479986]
18. Cruikshank WW, Kornfeld H, Center DM. Interleukin-16. J. Leukoc. Biol. 2000; 67:757–766. [PubMed: 10857846]
19. Cruikshank W, Center DM. Modulation of lymphocyte migration by human lymphokines. II. Purification of a lymphotactic factor (LCF). J. Immunol. 1982; 128:2569–2574. [PubMed: 7042841]
20. Cruikshank W, Little F. Interleukin-16: the ins and outs of regulating T-cell activation. Crit. Rev. Immunol. 2008; 28:467–483. [PubMed: 19265505]
21. Little FF, Lynch E, Fine G, Center DM, Cruikshank WW. Tumor Necrosis Factor- $\alpha$ -Induced Synthesis of Interleukin 16 in Airway Epithelial Cells. Am. J. Respir. Cell Mol. Biol. 2003; 28:354–362. [PubMed: 12594062]
22. Zhang Y, et al. Processing and activation of pro-interleukin-16 by caspase 3. J. Biol. Chem. 1998; 273:1144–1149. [PubMed: 9422780]
23. Aggarwal BB. Signalling pathways of the TNF superfamily: a double-edged sword. Nat. Rev. Immunol. 2003; 3:745–756. [PubMed: 12949498]
24. Wang P, et al. IL-16 Induces Intestinal Inflammation via PepT1 Upregulation in a Pufferfish Model: New Insights into the Molecular Mechanism of Inflammatory Bowel Disease. J. Immunol. 2013; 191:1413–27. [PubMed: 23817423]
25. Gomez MI, Seaghdha MO, Prince AS. *Staphylococcus aureus* protein A activates TACE through EGFR-dependent signaling. EMBO J. 2007; 26:701–709. [PubMed: 17255933]
26. Lavrik IN, Krammer PH. Regulation of CD95/Fas signaling at the DISC. Cell Death Differ. 2011; 19:36–41. [PubMed: 22075988]
27. Vaisid T, Barnoy S, Kosower NS. Calpain activates caspase-8 in neuron-like differentiated PC12 cells via the amyloid-beta-peptide and CD95 pathways. Int. J. Biochem. Cell Biol. 2009; 41:2450–2458. [PubMed: 19646546]
28. Chun J, Prince A. Activation of Ca<sup>2+</sup>-dependent signaling by TLR2. J. Immunol. 2006; 177:1330–1337. [PubMed: 16818794]
29. Takeuchi O, Hoshino K, Akira S. Cutting edge: TLR2-deficient and MyD88-deficient mice are highly susceptible to *Staphylococcus aureus* infection. J. Immunol. 2000; 165:5392–5396. [PubMed: 11067888]
30. Chae H. Molecular mechanism of staurosporine-induced apoptosis in osteoblasts. Pharmacol. Res. 2000; 42:373–381. [PubMed: 10987998]
31. Center DM, Cruikshank W. Modulation of lymphocyte migration by human lymphokines. I. Identification and characterization of chemoattractant activity for lymphocytes from mitogen stimulated mononuclear cells. J. Immunol. 1982; 128:2563–2568. [PubMed: 7042840]
32. Lynch EA, Heijens CAW, Horst NF, Center DM, Cruikshank WW. Cutting edge: IL-16/CD4 preferentially induces Th1 cell migration: requirement of CCR5. J. Immunol. 2003; 171:4965–4968. [PubMed: 14607889]
33. Glass WG, Sarisky RT, Vecchio AMD. Not-So-Sweet Sixteen: The Role of IL 16 in Infectious and Immune-Mediated Inflammatory Diseases. J. Interferon Cytokine Res. 2006; 26:511–520. [PubMed: 16881862]

34. Keane J, et al. Conservation of structure and function between human and murine IL 16. *J. Immunol.* 1998; 160:5945–5954. [PubMed: 9637508]
35. Wilson KC, Center DM, Cruikshank WW. The effect of interleukin-16 and its precursor on T lymphocyte activation and growth. *Growth Factors.* 2004; 22:97–104. [PubMed: 15253385]
36. Ren F, et al. Pro-IL-16 regulation in activated murine CD4+ lymphocytes. *J. Immunol.* 2005; 174:2738–2745. [PubMed: 15728482]
37. Parker D, Prince A. Immunopathogenesis of *Staphylococcus aureus* pulmonary infection. *Semin. Immunopathol.* 2012; 34:281–297. [PubMed: 22037948]
38. Hogan PG, Lewis RS, Rao A. Molecular basis of calcium signaling in lymphocytes: STIM and ORAI. *Annu. Rev. Immunol.* 2010; 28:491–533. [PubMed: 20307213]
39. Cohen TS, Prince AS. Bacterial pathogens activate a common inflammatory pathway through IFN $\lambda$  regulation of PDCD4. *PLoS Pathog.* 2013; 9:e1003682. [PubMed: 24098127]
40. Cohen TS, Prince AS. Activation of inflammasome signaling mediates pathology of acute *P. aeruginosa* pneumonia. *J. Clin. Invest.* 2013; 123:1630–1637. [PubMed: 23478406]
41. Archer NK, Harro JM, Shirtliff ME. Clearance of *Staphylococcus aureus* Nasal Carriage Is T Cell Dependent and Mediated through Interleukin-17A Expression and Neutrophil Influx. *Infect. Immun.* 2013; 81:2070–2075. [PubMed: 23529621]
42. Ahuja N, et al. Circulating IL-6 mediates lung injury via CXCL1 production after acute kidney injury in mice. *Am. J. Physiol. Renal Physiol.* 2012; 303:F864–72. [PubMed: 22791336]
43. Neumann B, et al. Mechanisms of acute inflammatory lung injury induced by abdominal sepsis. *Int. Immunol.* 1999; 11:217–227. [PubMed: 10069420]
44. Diep BA, et al. Complete genome sequence of USA300, an epidemic clone of community-acquired methicillin-resistant *Staphylococcus aureus*. *Lancet.* 2006; 367:731–739. [PubMed: 16517273]
45. Meagher C, et al. Neutralization of interleukin-16 protects nonobese diabetic mice from autoimmune type 1 diabetes by a CCL4-dependent mechanism. *Diabetes.* 2010; 59:2862–2871. [PubMed: 20693344]
46. Parker D, et al. *Streptococcus pneumoniae* DNA initiates type I interferon signaling in the respiratory tract. *MBio.* 2011; 2:e00016–11. [PubMed: 21586648]

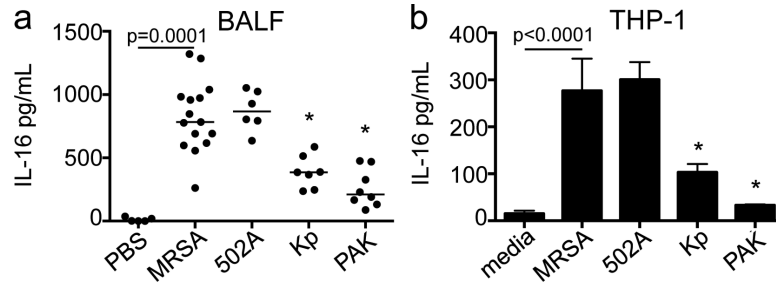


**Figure 1. *S. aureus* induces IL-16 production *in vivo* and *in vitro***

(a) C57BL/6J WT mice inoculated with  $10^7$  cfu of methicillin resistant *S. aureus* USA300 (MRSA), *S. aureus* 502A, *K. pneumoniae* ST 258 (Kp) or *P. aeruginosa* strain (PAK) or PBS. Bronchoalveolar lavage fluid(BALF) was obtained 24 hours after infection and quantitated by ELISA. Each dot represents an individual mouse; lines represent median values; data was compiled from 2 independent experiments. \* $p < 0.05$  as compared to MRSA, Student's *t* test, post hoc Dunnett's test. Lines represent median values. (b) THP-1s were stimulated with MRSA, *S. aureus* 502A, Kp or PAK (MOI 100) \* $p < 0.05$  compared to media, Student's *t*-test, post-hoc Dunnett's test. Graph shown is representative of 2 independent experiments.

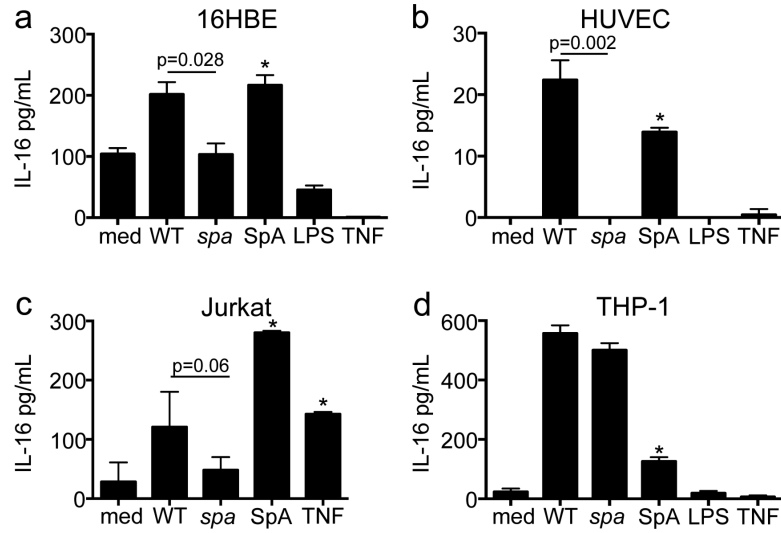


**Figure 2. IL-16 secretion is SpA specific in multiple cell types**

(a) 16HBEs, (b) HUVECs, (c) Jurkats and (d) THP-1s were infected with wt MRSA or *spa* mutant (MOI 100, 4h for 16HBEs, 2h for HUVECs, Jurkats and THP-1s). SpA, LPS, and TNF were added at a concentration of 0.5  $\mu$ M, 10  $\mu$ g/mL, and 100  $\mu$ g/mL respectively. IL-16 in culture supernatants was quantified by ELISA (\* $p$ <0.05 compared to media, Student's *t*-test, post-hoc Dunnett's test). Graphs represent data from at least 2 independent experiments.

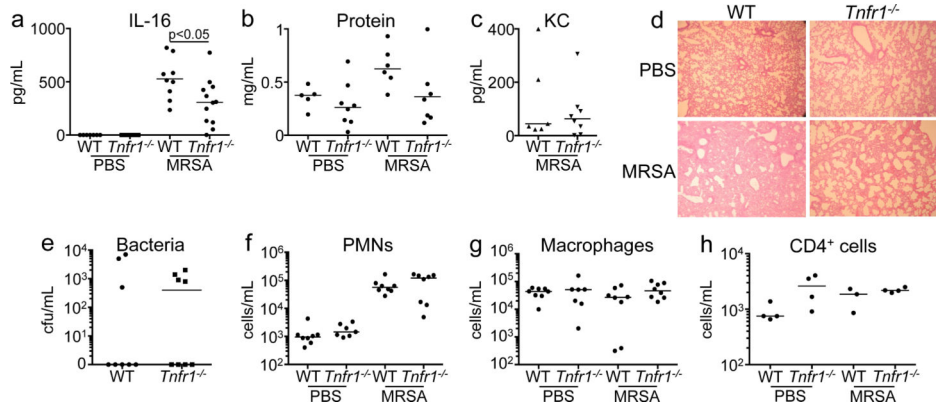


### Figure 3. TNFR1 is involved in IL-16 secretion

Age and sex matched cohorts of C57BL/6J WT and *Tnfr1*<sup>-/-</sup> mice were inoculated with  $10^7$  cfu of MRSA or PBS for 24 hours. BALF was quantitated for (a) IL-16 by ELISA, (b) total protein (c) and KC by ELISA. (d) H&E sections of fixed whole lungs. Magnification 100x. (e) Bacterial cfus were counted in BALF. (f) Neutrophils (PMNs) ( $\text{Ly6G}^+/\text{MHCII}^-$ ) and (g) Macrophages ( $\text{CD11c}^+/\text{MHCII}^{\text{low-mid}}$ ) in the BALF, as well as  $\text{CD4}^+$  cells in lung homogenate (h) were enumerated by flow cytometry. Each dot represents an individual mouse and is compiled from 3 independent experiments. Lines represent median values.

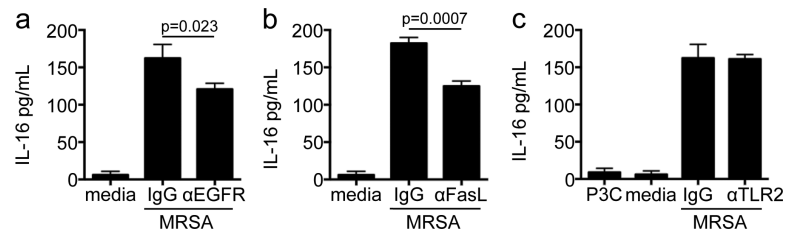


**Figure 4. Multiple receptors are involved in MRSA induced IL-16 secretion in THP-1s**  
 THP-1s were pretreated with neutralizing antibody or IgG isotype 1 hour prior to infection with MRSA at a MOI of 50. Neutralizing antibodies were (a) anti-EGF receptor (EGFR) (2  $\mu$ g/mL), (b) anti-FasL (5  $\mu$ g/mL) and (c) anti-TLR2 (2  $\mu$ g/mL). Pam<sub>3</sub>Cys-Ser-Lys<sub>4</sub> (P3C) (15 $\mu$ g/mL) was used as a control. p values as compared to isotype controls, Student's *t*-test. The above graphs represent data from at least 2 independent experiments.

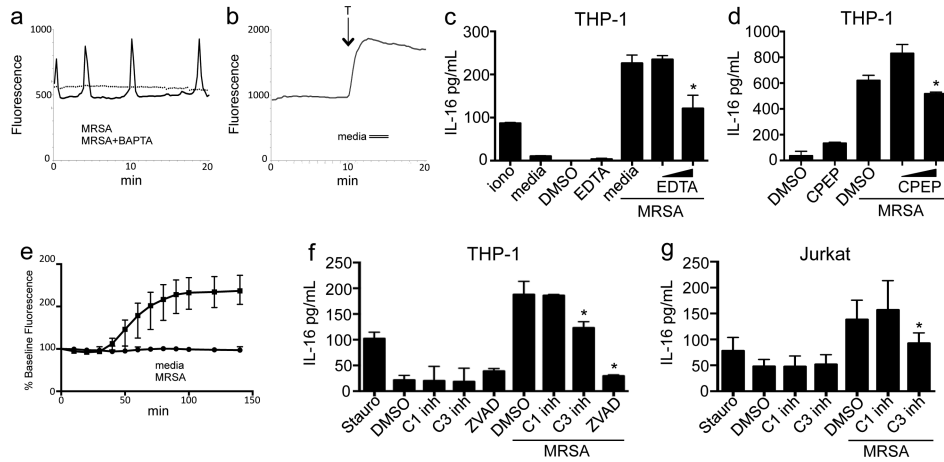


**Figure 5. MRSA induction of IL-16 release is calcium and calpain dependent in THP-1s**  
 Calcium fluxes were measured by fluorescence activation on an inverted microscope with a GFP mercury laser. THP-1s loaded with AM/Flo-4 (1mM) and PowerLoad concentrate (1mM) 2 hours prior to stimulation with (a) MRSA (MOI 100) with and without BAPTA (6 $\mu$ M), or (b) media alone followed by thapsigargin (1 $\mu$ M) (T) as a positive control. Representative cells were chosen and fluorescence plotted over time. (c) IL-16 levels in supernatants of THP-1s pretreated 1 hour prior to infection with EGTA (0.5 or 1mmol) with MRSA (MOI 50) was measured 2 hours after infection. (d) IL-16 levels in supernatants of THP-1s pretreated 1 hour prior to infection with calpeptin (CPEP) (20 or 200  $\mu$ M) with MRSA (MOI 50) was measured 2 hours after infection. Ionomycin (iono) in DMSO was 5 mM. (e) THP-1s were preloaded with Caspase-3/7 Green Detection agent (5 $\mu$ M) 30 minutes prior to infection and then infected with MRSA (MOI 100). Fluorescence was then plotted over time. (f) IL-16 levels in supernatants of THP-1s were pretreated 1 hour prior to infection with respective inhibitor with MRSA (MOI 50) for 2 hours; caspase 1 inhibitor (C1 inh) 50  $\mu$ M, caspase-3 inhibitor (C3 inh) 50  $\mu$ M, and pan-caspase inhibitor (ZVAD) 100  $\mu$ M. Staurosporine in DMSO was 1 $\mu$ M. (g) IL-16 levels in supernatants of Jurkats were pretreated 1 hour prior to infection with respective inhibitor with MRSA (MOI 50) for 2 hours; caspase 1 inhibitor (C1 inh) 50  $\mu$ M and caspase-3 inhibitor (C3 inh) 50  $\mu$ M. Staurosporine in DMSO was 1 $\mu$ M. \* $p$ <0.05 value as compared to MRSA infected samples, Student's *t*-test, post-hoc Dunnett's test for multiple comparisons. The above graphs represent data from at least 2 independent experiments.

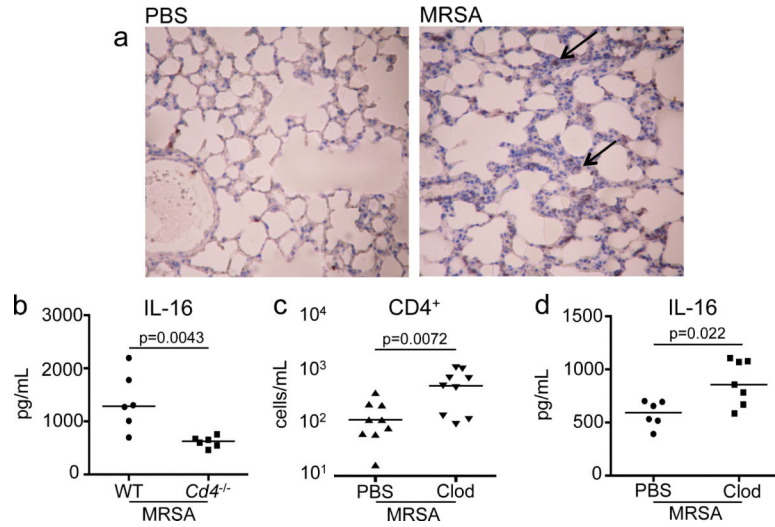


**Figure 6. IL-16 is produced by CD4<sup>+</sup> cells**

(a) Immunohistochemistry by standard methods with anti-IL-16 antibody on fixed whole lungs of C57BL/6J WT given PBS or infected with 10<sup>7</sup> MRSA for 24 hours. Magnification 100x. Black arrows point to areas of IL-16 staining (brown). (b) Age and sex-matched cohorts of C57BL/6J WT or *Cd4*<sup>-/-</sup> mice were inoculated intranasally with 10<sup>7</sup> MRSA and IL-16 was quantified in BALF collected by ELISA. Clodronate (Clod) or PBS liposome treated mice were given 10<sup>7</sup> MRSA for 24 hours. BALF stained for (c) CD4<sup>+</sup> populations were analyzed by flow cytometry and (d) IL-16 was measured by ELISA. Each dot represents an individual mouse and data is combined from 2 separate experiments. Lines represent median values.

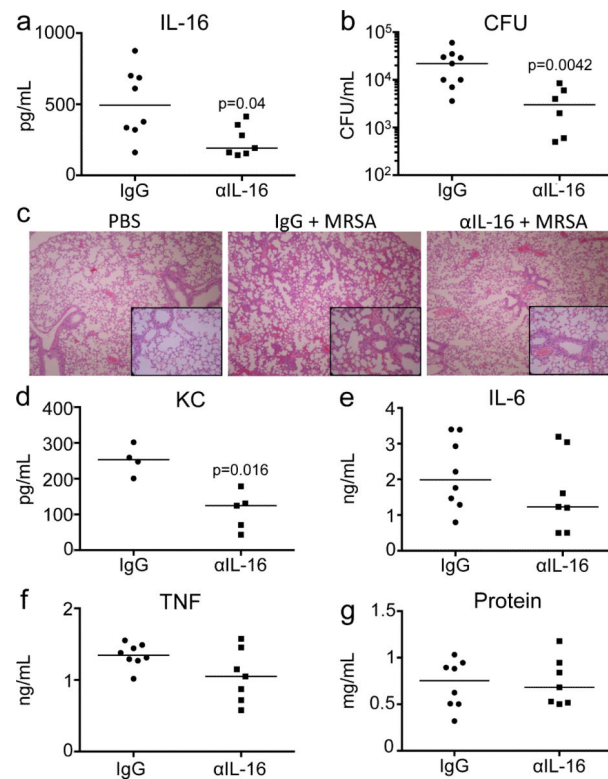


### Figure 7. Neutralization of IL-16 improves clearance of MRSA

Anti-IL-16 antibody or IgG isotype control was injected i.p. (100  $\mu$ g) 2 hours prior to infection with 10<sup>7</sup> cfu MRSA. Effect of IL-16 neutralization was documented by quantifying (a) IL-16 by ELISA and (b) bacterial clearance was measured by cfus in the BALF after 18 hours. (c) H&E sections of fixed whole lungs. Magnification 100x, inset box 400x. Cytokines (d) KC, (e) IL 6 and (f) TNF, as well as (g) protein were measured in the BALF. p values are as shown, as compared to IgG isotype, by Student's *t*-test. Each dot represents an individual mouse and data is combined from 2 separate experiments. Lines represent median values.